PROSTHETICS

Neural prosthesis control restores near-normative neuromechanics in standing postural control

Aaron Fleming[1,2], Wentao Liu[1,2], He (Helen) Huang[1,2]*

Current lower-limb prostheses do not provide active assistance in postural control tasks to maintain the user's balance, particularly in situations of perturbation. In this study, we aimed to address this missing function by enabling neural control of robotic lower-limb prostheses. Specifically, electromyographic (EMG) signals (amplified neural control signals) recorded from antagonistic residual ankle muscles were used to drive a robotic prosthetic ankle directly and continuously. Participants with transtibial amputation were recruited and trained in using the EMG-driven robotic ankle. We studied how using the EMG-controlled ankle affected the participants' anticipatory and compensatory postural control strategies and stability under expected perturbations compared with using their daily passive devices. We investigated the similarity of neuromuscular coordination (by analyzing motor modules) of the participants, using either device in a postural sway task, to that of able-bodied controls. Results showed that, compared with their passive prosthesis, the EMG-controlled prosthesis enabled participants to use near-normative postural control strategies, as evidenced by improved between-limb symmetry in intact-prosthetic center-of-pressure and joint angle excursions. Participants substantially improved postural stability, as evidenced by a reduction in steps or falls using the EMG-controlled prosthetic ankle. Furthermore, after relearning to use residual ankle muscles to drive the robotic ankle in postural control, nearly all participants' motor module structure shifted toward that observed in individuals without limb amputations. Here, we have demonstrated the potential benefit of direct EMG control of robotic lower limb prostheses to restore normative postural control strategies (both neural and biomechanical) toward enhancing standing postural stability in amputee users.

INTRODUCTION

Individuals with lower-limb amputation lose agency in their limb to interact with their everyday environments. Amputees relearn to navigate the world with prosthetic devices that are often mechanically passive, with a predetermined stiffness designed primarily for storing and returning energy. Amputee daily life, however, contains many activities that require active generation of energy at the missing limb, and their prosthetic device provides no active support during these tasks (e.g., picking up a child or shuffling in a line). The typical postural control strategy observed in able-bodied (AB) individuals, that is, ankle strategy (*1*), is no longer an option on the amputated side, limiting the user's postural control options and standing stability (the ability to maintain balance) (*2*). Other postural control mechanisms, such as center-of-pressure to center-of-mass relationship (*3*) and dynamic balance contribution (*4*), are compromised when individuals use typical passive prosthetic ankles, likely contributing to poorer postural control compared with AB individuals (*5*, *6*). Clinical measures of balance and functional task performance in lower-limb amputees are associated with higher incidence of falls (*7*, *8*); this population also has lower balance confidence and participates less in their community (*9*, *10*). Further, amputees often develop neuromuscular and biomechanical compensation strategies (*11*, *12*) that rely more heavily on their intact limb and joints, which create long-term consequences, such as higher risk for osteoporosis, arthritis, and pain (*13*).

Recent advances in robotic lower limb prostheses, which can generate active torque (*14*–*18*), present great promise to further address mobility and stability in individuals with lower-limb amputations. A majority of existing research efforts have been spent on autonomous robotic prosthesis control to restore normative walking (*15*, *19*). These autonomous control paradigms often rely on onboard sensors in the prosthetic device to estimate human state and then reactively deliver predetermined joint mechanics. This control is suited for biomechanically well-defined, predictable motor behaviors, such as cyclic walking on different terrains or with different speeds (*20*, *21*). However, such autonomous control is ill-suited to generate proactive prosthesis actions for contexts that require preparatory adjustments, such as anticipatory postural adjustments (APAs), or require full body coordination that is difficult to predefine, such as compensatory postural adjustments (CPAs). These postural control mechanisms constitute the building blocks for many daily life tasks. APAs are crucial for maintaining balance, as evidenced by significant changes in stability when individuals know a perturbation is impending versus when they are blinded to the timing (*22*, *23*). These volitional, feedforward actions (not generated through reflexive neural commands) alleviate the burden on CPAs, which are responsible for maintaining balance after a perturbation has already occurred (*23*, *24*). Improvement of these mechanisms could likely improve clinical outcomes, as evidenced by a previous study with elderly individuals (*25*). Hence, control mechanisms to further improve the function of robotic lower limb prostheses to address anticipatory and CPAs for assisting versatile activities, beyond steady-state walking, are needed.

One potential solution is to directly integrate the prosthesis control with efferent neural commands of amputee users. Electromyographic (EMG) signals recorded from the residual muscles have

[1]Joint Department of Biomedical Engineering, North Carolina State University, Raleigh, NC 27695, USA. [2]Joint Department of Biomedical Engineering, University of North Carolina at Chapel Hill, Chapel Hill, NC 27599, USA.
*Corresponding author. Email: hhuang11@ncsu.edu

been widely used as a neural control source for prosthetic limbs (*26*), because EMG signals are amplified motor control signals and because amputees retain the ability to generate feedforward activations of their residual muscles (often eliciting a sensation of moving a "phantom limb") (*27*). Research groups have used EMG pattern recognition to recognize the user's locomotion mode for terrain-adaptive lower-limb prosthesis control (*28*–*30*). An EMG-based neural interface was used as a supervisory controller to select the appropriate autonomous prosthesis control according to the user-intended locomotion mode (level ground walking, stair ascent and descent) (*31*). Because this paradigm relies on preprogrammed autonomous control to operate a prosthesis, it is still difficult to address postural control tasks. Another neural control paradigm, called direct EMG (dEMG) control (*31*), uses neuromuscular activity of residual muscles that originally controlled the amputated joint to directly and continuously modulate an artificial joint's mechanics. This control paradigm follows the biological process for limb movement production, restores the biomechanical influence of residual muscle activation (*31*–*34*), and enables individuals to continuously operate their prosthetic joint based on the neural control commands in humans, just like control of an intact joint. Hence, this control paradigm allows the amputee user to operate the prosthesis joint directly and freely in a variety of tasks, including anticipatory and compensatory postural control.

A few studies tested dEMG control paradigm on lower-limb amputees to operate a virtual object in a sitting position (*27*, *35*, *36*) or a robotic lower-limb prosthesis (*32*, *37*–*39*). These existing studies observed the initial difficulty of individuals with limb amputations in using dEMG control and their capability to adapt the residual muscle activity for successful prosthesis operation after training (*27*, *32*, *35*–*39*). The initial difficulty is potentially caused by altered residual muscle activation patterns due to limb amputation (*40*–*42*) and change of dynamics from a biological limb to a prosthesis or a virtual system. However, through practice, amputee participants can adapt their coordination of residual muscle activity and reestablish the relationship between neural control commands and the resulting state change of the controlled device for successful task performance. The duration of the practice ranged from less than an hour in a single experimental session (*27*, *35*, *36*) to a few sessions in multiple lab visits (*32*, *37*, *39*); thus, it is unclear whether additional training may elicit greater improvements. These results indicate the feasibility and promise of dEMG control for lower-limb prostheses. Nevertheless, there were also limitations in these preliminary studies on dEMG prosthesis control. First, except for our prior single case study that investigated postural control in quiet standing (*39*), almost all of the existing studies that applied dEMG control to a physical prosthesis focused on locomotive task testing (*32*, *34*, *43*, *44*). Because autonomous control has been implemented in robotic lower-limb prostheses to successfully assist locomotive tasks, these studies of dEMG control have not brought additional functionality into the existing robotic prostheses. Second, the existing studies focused the evaluations on the residual muscle activity and dynamics of prosthetic joints during the task performance to show the feasibility of dEMG prosthesis control. Little attention has been given to the potential influence of dEMG prosthesis control on multijoint and multimuscle coordination. Because gait and posture involve dynamics and coordination among many body segments, it is important to understand how the activity of residual muscles, after restoring their biomechanical influence, and resulting prosthesis mechanics are integrated and coordinated with the intact human body to complete tasks in locomotion or postural control.

Therefore, the goal of our research is to address the need to advance robotic prosthesis function for active assistance of postural control and stability of lower limb amputee users through dEMG control. Specifically, in this study, we systematically investigated the influence of dEMG control of a robotic ankle on the amputee users' standing stability and biomechanics and neuromuscular coordination in postural control tasks (Movie 1). We recruited and trained individuals with transtibial amputations (TT) in using a dEMG-controlled, pneumatic muscle–driven robotic prosthetic ankle in several postural control tasks first. Then, we evaluated the participants with untrained tasks. First, a specially designed anticipatory postural perturbation platform was used to quantify the

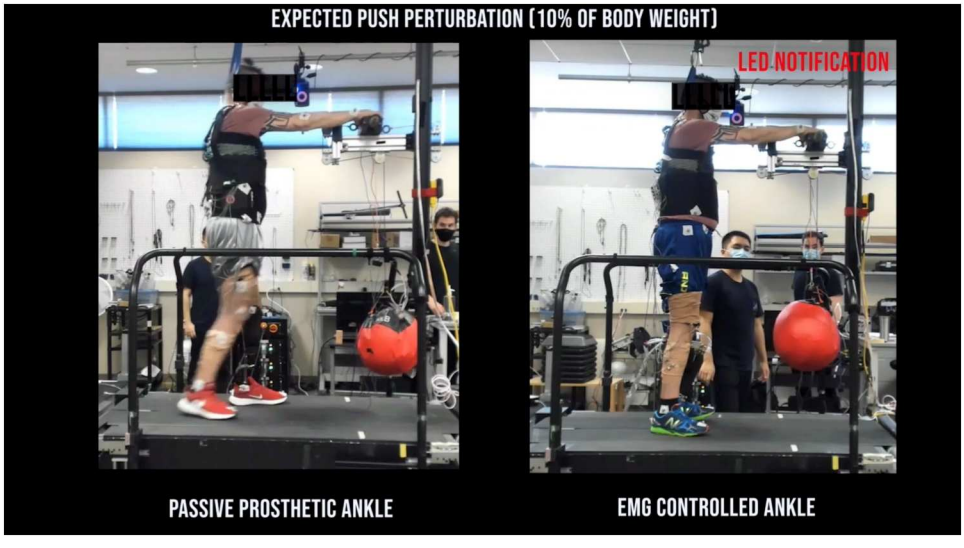

Movie 1. Summary of the methods and results.

biomechanics of APA and CPA and postural stability of amputee participants when using a dEMG-controlled prosthesis compared with their daily devices. Next, to evaluate dEMG prosthesis control on neuromuscular coordination, we investigated activity of lower-limb muscles in both intact and amputated limbs during a voluntary postural sway task (*45*). The neuromuscular coordination was quantified by motor modules, a commonly used method to quantify neuromechanical solutions for producing coordinated body motion such as gait and posture (*46*, *47*). To our knowledge, addressing robotic prosthesis function on postural stability and balance is important for the amputee users' daily task performance but has not been demonstrated in the field. The results of this study can contribute important knowledge on the potential benefit of dEMG control of robotic lower-limb prostheses on restoring near-normal postural control capability in lower-limb amputees for improved stability. We expect the improvement of postural control and stability to accomplish daily life activities via modern robotic prosthesis technology to have an effect on the quality of life for amputees by empowering them to participate in many more areas of life in the future.

RESULTS

We recruited five TT individuals to participate in this study [five males, age: 43.4(±11.72) mean (SD) years] and five AB participants [five males, age: 39.2(±11.43) years]. Additional information about the five TT participants is provided in Table 1 (Materials and Methods). All TT participants were active, community ambulators who wore their prosthesis at least 12 hours a day. TT participants underwent training with the dEMG-controlled device; then, they were evaluated using an expected perturbation platform that applied disturbances to participants via the arms (Fig. 1), similar to the previous study of anticipatory and CPAs (*23*, *48*–*50*). Participants also conducted a voluntary postural sway task (postural sway task was trained). TT participants were evaluated using their daily, passive device and, on a separate day, using the dEMG-controlled prosthetic ankle. AB participants were evaluated on a single day. We evaluated participants' stability under expected perturbation with a body weight (BW)–normalized perturbation at the shoulder level for two directions (10% BW push, 10% BW pull) with five repetitions for each direction. We evaluated participants' neuromuscular coordination strategy using a voluntary sway task where participants swayed as far forward and backward as possible while keeping their feet flat on the ground for 25 consecutive sways (*45*). We measured joint kinematics and kinetics using full-body motion capture and an instrumented split-belt treadmill. We measured electromyography from the lower limbs.

Table 1. Amputee participant demographics.

Participant	Age (years)	After amputation (years)	Reason for amputation
TT1	58	9	Soft tissue sarcoma
TT2	41	18	Trauma
TT3	32	15	Trauma
TT4	53	6	Trauma/failed limb salvage
TT5	33	0.75	Dysvascular

Neural control of robotic ankle enabled symmetrical, synchronized bilateral limb mechanics

To evaluate participants when using a dEMG-controlled prosthesis (dEMG) compared with when using their daily passive device (passive) under expected perturbation (an untrained task), we developed and used a custom perturbation platform (Figs. 1 and 2A). In both expected pull and push perturbation conditions, we observed noticeable improvements in stability measures of TT participants for the dEMG condition compared with the passive condition. Under these conditions, participants generated anticipatory adjustments of their center of mass (CoM) against the direction of the perturbation. During the "push" condition, the AB participants moved their CoM in the anterior direction (negative) before the weight was released and continued to hold their CoM forward well after perturbation (Fig. 2B). At the moment of release (t = 0

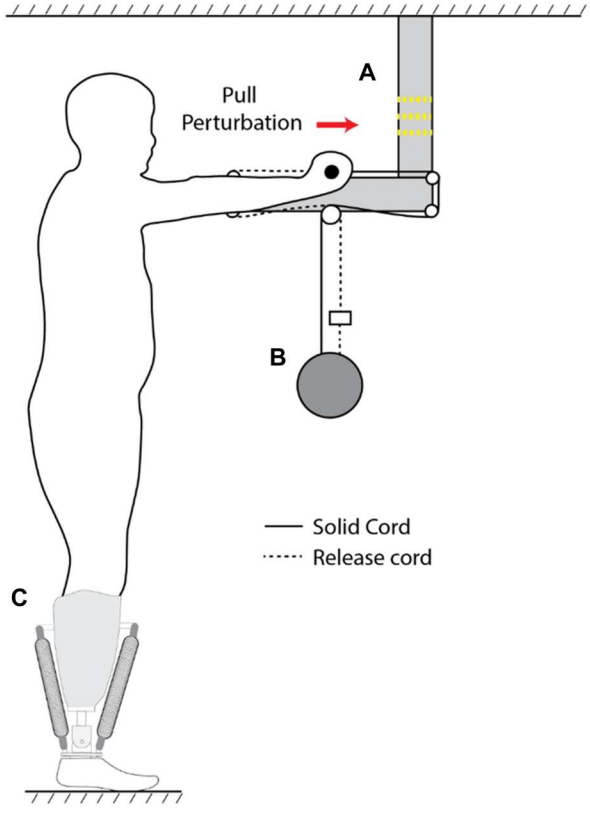

Fig. 1. Experimental platform illustration. Participant stands upright while holding a handle bar at arm's length and shoulder height. The handlebar is attached to a suspended weight by two cords. One cord is directly attached to the weight (solid line, solid cord), and the other is attached to the weight with an electromagnet in series that, when switched off, severs the cord's connection with the weight (dashed line, release cord). In this illustration, the perturbation platform delivers a pulling perturbation on the participant. The direction of the perturbation is switched by alternating the respective locations of the solid and release cords. (**A**) LED light. The LED light is switched off 0.6 s before the electromagnet is released, providing the participants with a notification of the impending perturbation. (**B**) Perturbation load. Weight for both push and pull conditions is normalized to 10% of the participant's BW. (**C**) Pneumatic artificial prosthetic ankle.

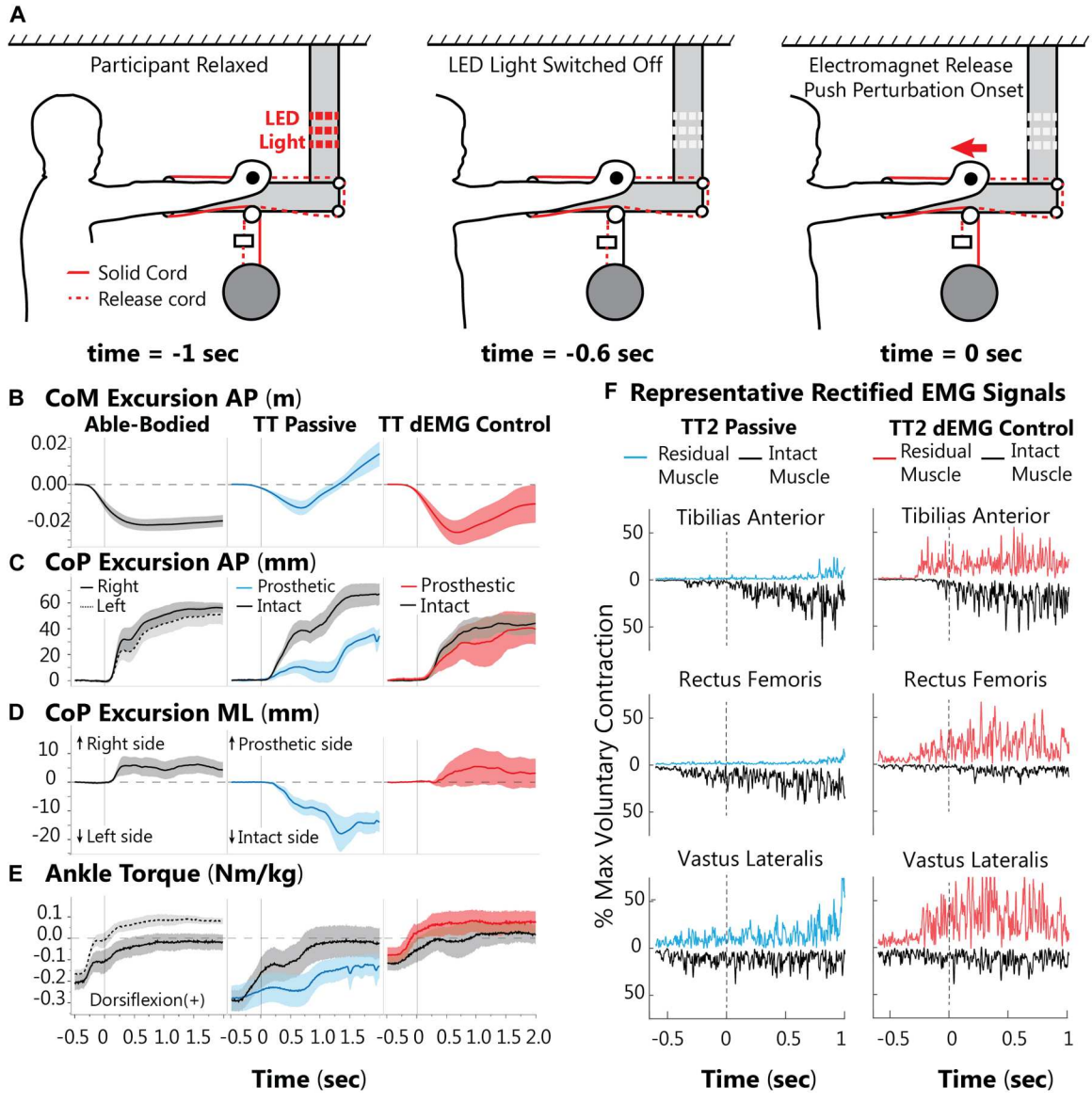

Fig. 2. Average AB and TT participant responses to pushing perturbation. Perturbation magnitude is normalized to 10% BW. TT participants were tested with their passive device and a dEMG control prosthetic ankle. (**A**) Example expected push perturbation setup. Before each trial, the participant is relaxed. The light is then switched off, indicating that the ball will release in 0.6 s. At the time of release, the release cord is severed, and the participant is pushed with the perturbation load. (**B**) AP CoM excursion for AB (solid and dashed lines are right and left foot, respectively), TT with daily, passive device (blue), and TT dEMG control (red) posttraining (black line for intact limb in both conditions). (**C**) AP CoP excursion. (**D**) ML CoP excursion. (**E**) Ankle joint torque for both limbs. (**F**) Representative trial of EMG activity with passive and dEMG control. For display purposes, only residual EMG activity is shown on the positive axis (red), and we flipped the intact EMG activity about the horizontal axis (black). Both signals are positive. For (B) to (E), shaded areas represent SE across participants.

s), AB participants had more anticipatory CoM excursion than the passive ($P = 0.012$; $P < 0.05$ is considered significant) but not the dEMG condition ($P = 0.092$) (Fig. 2B). During the compensatory "hold" time (average value during $t = 1$ to 2 s), we observed similar CoM excursion between AB and TT participants with dEMG control ($P = 0.516$) but not with their passive daily device ($P = 0.004$).

TT participants also improved center of pressure (CoP) excursion in the anterior-posterior (AP) and medial-lateral (ML) directions using dEMG control compared with their daily passive device for the pushing perturbation (Fig. 2, C and D, respectively). In their daily device, TT participants generated anticipatory CoP excursion with their intact foot at $t = 0$ s in the posterior direction; however, the CoP excursion under the passive prosthetic foot remained significantly less [release: 31.48(±14.62 mm) versus 6.94(±8.46 mm), $P = 0.005$]. To evaluate compensation from the perturbation, the CoP excursion was averaged during a hold period after the perturbation, defined as $t = 1$ to 2 s. The difference of CoP excursion between the intact and prosthetic foot was not significant after the perturbation [hold: 61.17(±26.72 mm) versus 38.17(±13.33 mm), $P = 0.210$]. Using dEMG control, TT participants generated symmetrical CoP excursion between their intact and prosthetic foot

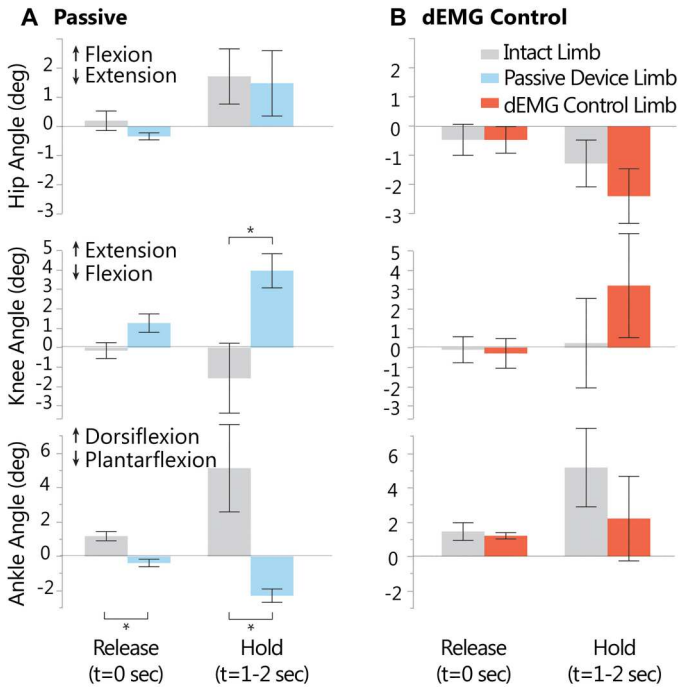

Fig. 3. Anticipatory and compensatory joint angle excursion during the push condition. (**A**) Ankle, knee, and hip joint excursion (relative to standing at rest, t = −0.6 s to −0.5 s) during passive device condition at release time point (t = 0 s) and hold time point (average angle during 1- to 2-s postperturbation). (**B**) Joint angle excursions (relative to standing at rest) with dEMG control, posttraining, for release and hold time points. Knee and ankle joint excursion differed significantly between limbs in the passive but not the dEMG control condition. Each bar represents the mean value, and the error bars denote SE from the mean. Positive excursion represents flexion for the hip joint, extension for the knee joint, and dorsiflexion for the ankle joint. Significant differences (P < 0.05) are denoted by *.

for both time points [release: 24.96(±18.29 mm) versus 20.05(±16.12 mm), P = 0.509; hold: 48.66(±14.96 mm) versus 33.61(±23.40 mm), P = 0.210]. We observed similar symmetry of CoP excursion in AB participant behavior (Fig. 2, C and D). In the ML direction with their daily passive device, TT participants demonstrated anticipatory CoP ML excursion toward their intact limb [release: −5.68(±4.18 mm)] and similar compensatory CoP ML excursion [hold: −12.08(±7.02 mm)]. However, with the dEMG control, participants moved CoP ML toward their prosthetic in anticipatory [release: 1.93(±7.99 mm)] and compensatory time points [hold: 2.69(±11.60)]. These CoP ML excursions were significantly different between passive and dEMG conditions for the compensatory time point (hold: P = 0.036) but not for the anticipatory time point (release: P = 0.154). Using the dEMG control, participants had similar magnitude CoP ML excursions compared to our AB control participant (Fig. 2D) (release: P = 0.855, hold: P = 0.721). Results for the pull condition can be viewed in the Supplemental Materials (fig. S1).

Before the perturbation, AB individuals had a resting plantarflexion torque (Fig. 2E, t = −0.5 s) and generated an anticipatory change in torque before perturbation. Shortly after perturbation onset (t = 0 s), individuals generated dorsiflexion torque primarily with their right leg. Using dEMG control, TT participants generated similar levels of torque from both their prosthetic and intact limbs. However, using their passive device, individuals did not generate dorsiflexion torque with their prosthetic limb and had delayed generation of dorsiflexion with their intact limb (Fig. 2E). Representative EMG from TT2 participant also demonstrated differing activation patterns between the residual and intact tibialis anterior (TA) muscles (Fig. 2F). Using their passive device, TT2 generated anticipatory activation of intact shank and thigh muscles but did not noticeably activate their residual TA or rectus femoris. Using dEMG control, TT2 significantly activated both residual and intact limb shank and thigh muscles (Fig. 2F).

Neural control of robotic ankle enabled matched intact and residual limb joint motions

We observed that TT participants modified postural configuration and overall joint strategies when using dEMG control to match their intact limb more closely in both "push" and "pull" conditions (Fig. 3 and tables S1 and S2). At the release of the push perturbation, the participants actuated their intact and prosthetic ankle in opposing directions while using their daily passive device (Fig. 3A, P = 0.0007). However, we observed no difference in joint angle excursions between intact and dEMG-controlled prosthetic ankles (P = 0.487). During the perturbation hold (t = 1 to 2 s), we observed a significant difference between intact and prosthetic ankle joint excursions in the passive but not the dEMG control condition (passive: P = 0.005; dEMG: P = 0.195). We did not observe a significant difference between intact and residual knee joint excursions in the passive condition at the release point (Fig. 3A, P = 0.060); however, this result approached significance. We did not observe interlimb differences in the dEMG control condition for the same time point (Fig. 3B, P = 0.8345). We observed a significant difference between the intact limb knee joint and residual limb knee joint during the perturbation hold for only the passive condition [passive: −1.57°(±4.03°) versus 3.96°(±1.97°), P = 0.037] and not the dEMG control condition [0.23°(±5.15°) versus 3.20°(±6.00°), P = 0.1437, and these values indicate mean (±SD)]. For hip joint comparisons, we only observed no significant difference between limbs for the passive condition or dEMG control condition at release or hold time points.

dEMG control of robotic ankle normalized postural control strategy and reduced falls and compensatory steps in participants

We observed distinct changes in balancing strategies as TT participants used dEMG control compared with their passive device (Fig. 4). While using dEMG, three TT participants used predominantly an ankle joint strategy, as evidenced by relatively small excursions from the knee and hip joint and a large, synchronized excursion from the ankle joints (Fig. 4A). We observed that two TT participants used a mixed strategy, with simultaneous excursion from all joints (Fig. 4B). These participants still improved synchronization between prosthetic and intact limb ankle joint excursion compared with their passive device. Overall, nearly all participants failed to maintain static standing balance at least once (participants took a step or allowed handlebar to reach the end of the track) while using their passive device. Although one participant still failed to maintain balance in some repetitions using dEMG control only, all remaining participants were able to maintain static standing balance (Fig. 4C).

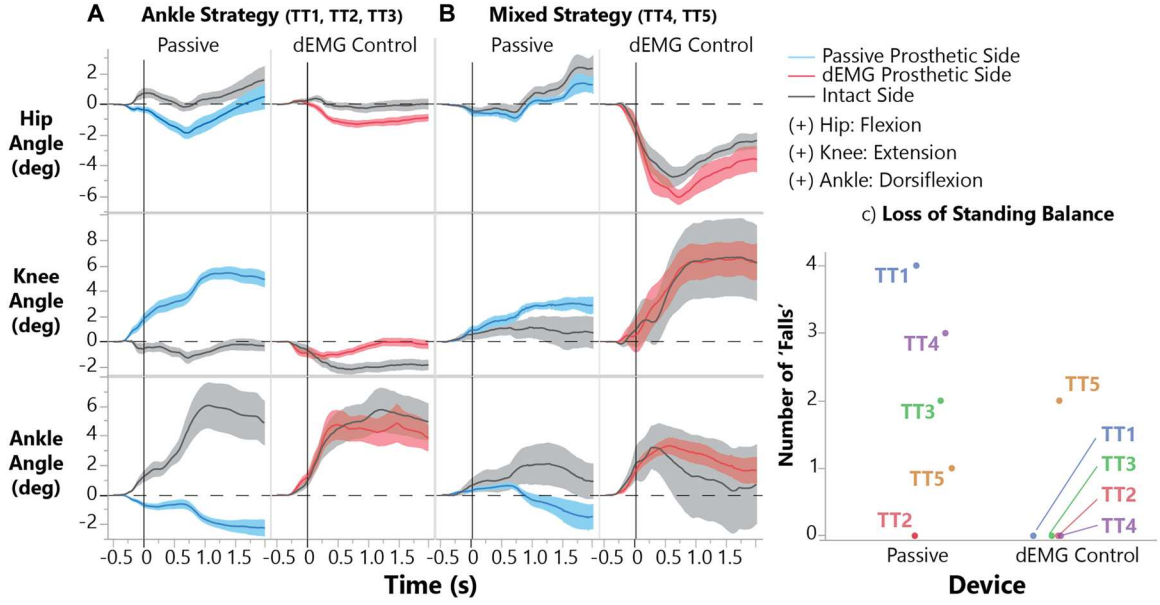

Fig. 4. Balance strategies during pushing perturbation with passive and dEMG control prosthetic ankles. (**A**) Amputee participants (TT) who used an "Ankle" strategy (knee and hip joint excursion <2°, see Materials and Methods) and significantly increased prosthetic ankle joint dorsiflexion using dEMG control. (**B**) TT participants that used a "Mixed" postural control strategy with the dEMG-controlled prosthetic ankle during perturbation (hip, knee, and ankle joint excursions >2°, see Materials and Methods). Shaded areas represent SE. (**C**) Number of trials where individual participants could not maintain balance, resulting in a step or allowing the handlebar to reach the end of the provided track.

dEMG control resulted in near-normative neural coordination patterns

To study neural coordination, participants were also asked to perform postural sway task while EMG signals were recorded from bilateral muscles of lower limbs. To illustrate neural coordination changes on an individual basis, we plotted muscle module structures and activation coefficients from one representative AB participant (AB1) and one representative TT participant (TT5) using their daily, passive device and the dEMG control (Fig. 5). Using TT5 as our representative participant, we observed noticeable contribution from a single anterior muscle when TT5 used their passive device (intact rectus femoris had the highest contribution in muscle module, although predominantly posterior muscles were activated; Fig. 5A), and this contribution was notably less when using the dEMG control prosthetic ankle. For 'backward' muscle modules, TT5 generated two muscle modules (Fig. 5B); however, TT5 used only one module with the dEMG control. This muscle module used in the dEMG condition was notably similar to that observed in AB participants (AB1 as a representative example in Fig. 5) for both the muscle module structure and the activation coefficient.

We observed that nearly all TT participants used muscle module structures similar (r value above 0.735 significance level) to those of AB participants when using the dEMG-controlled prosthetic ankle (Fig. 6). Using their passive, daily device, only 3 of 12 muscle module structures across participants were significantly correlated to average AB module structure. Except for TT4, all participants demonstrated muscle module structures using dEMG control that were similar to AB behavior. Six of 11 muscle modules were above the significance threshold ($r > 0.735$), and three modules were close to significance (TT1: 0.69, TT3: 0.70, and TT3: 0.72). Three muscle modules were not included in this analysis because they were not labeled as a "Backward" or "Forward" sway (TT1 passive, TT2 passive, and TT1 dEMG control). One participant, TT4, did not show muscle module structure similar to AB behavior in either passive or dEMG control conditions. Each muscle module from Backward Sway from TT4 primarily contained muscles from a single leg (one module for residual limb muscles and one module for intact limb muscles). Thus, although the individual correlations for each of these muscle modules for TT4 was low compared with AB Backward modules, TT4 grouped residual muscle activity with activity from other muscles on the residual limb. All muscle modules for TT participants and the averaged muscle module structure for AB participants can be seen in supplementary figures (figs. S4 to S6).

DISCUSSION

In this study, we presented dEMG control of a robotic lower-limb prosthesis to enable modern robotic prostheses to actively assist postural stability of individuals with lower limb amputations, which has not been demonstrated previously. Unlike conventional therapeutic interventions in clinics that aim to improve strength and compensatory strategies of intact joints of lower limb amputees in postural control (*51*), we developed neural control of a robotic ankle prosthesis that enables the amputee users to restore normative postural control mechanisms, such as ankle strategy, for enhanced postural stability. We showed that dEMG control was reliable, partly because the information used in EMG signals for prosthesis control were the low-pass–filtered, smoothed EMG envelopes. All the participants using the dEMG-controlled ankle demonstrated marked improvement in standing stability, interlimb symmetry, and neuromuscular coordination strategy. All participants coordinated antagonistic residual muscle activity for prosthesis ankle

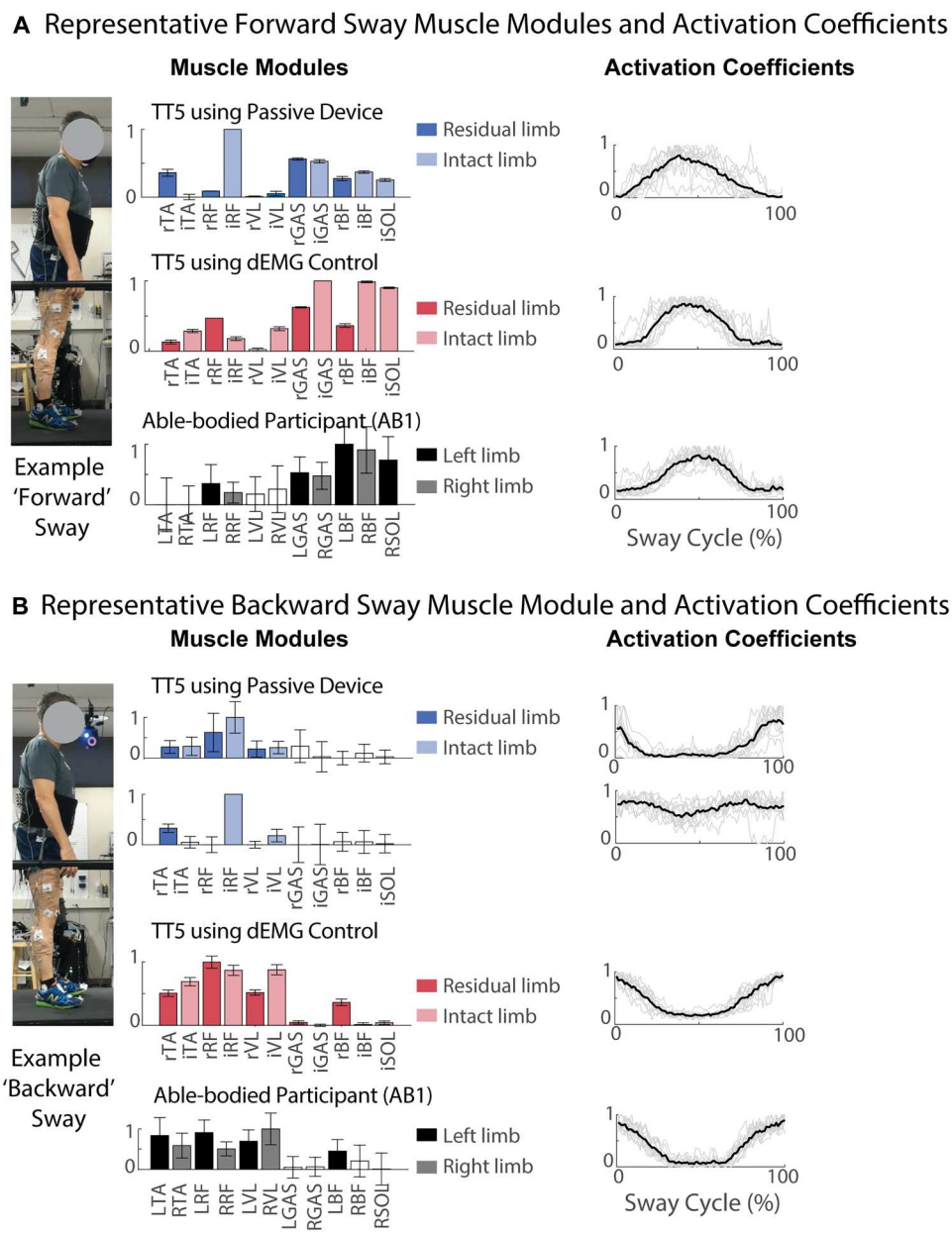

Fig. 5. Representative participant muscle module structure and activation coefficients. (**A**) Representative muscle module structures and activation coefficients for "forward" sway module for AB participant 1 (AB1, black bars) and a representative amputee participant (TT5) using the dEMG control prosthetic ankle (red bars) and their daily passive device (blue bars). (**B**) Representative muscle module structure and activation coefficient for backward sway modules. Muscle module structures display bars with average activation, and error bars indicate 95% confidence intervals for each muscle (muscles with white bars had 95% confidence interval falling below 0 and were considered inactive). Activation coefficients display activation for the respective muscle modules across time as a percentage of the sway cycle (mean and individual repetitions as black and gray lines, respectively). Muscle labels are as follows: Lowercase prefixes "r" and "i" represent residual and intact limbs, respectively. Uppercase prefixes L and R represent left and right limb for AB participants.

control, largely synchronizing intact and residual limb behavior in both expected perturbation and voluntary postural sway. Our results underscored the importance in incorporating continuous human efferent neural control into prosthesis operation to further broaden the functions of robotic prostheses beyond locomotion assistance and to improve standing stability in lower limb amputees.

One of the primary findings of this study was that, by enabling neural control of a robotic prosthetic ankle, amputees were capable of eliciting motor commands that synchronized several measures between intact and residual limbs and chose to use this synchronized interlimb behavior as a strategy during expected perturbation and voluntary postural sway. This symmetry was apparent in several measures, including CoP excursions and joint excursions in the ankle, knee, and hip. We first observed drastically improved CoP excursions during the push condition, where intact and residual limb behavior did not differ while using the dEMG control. This

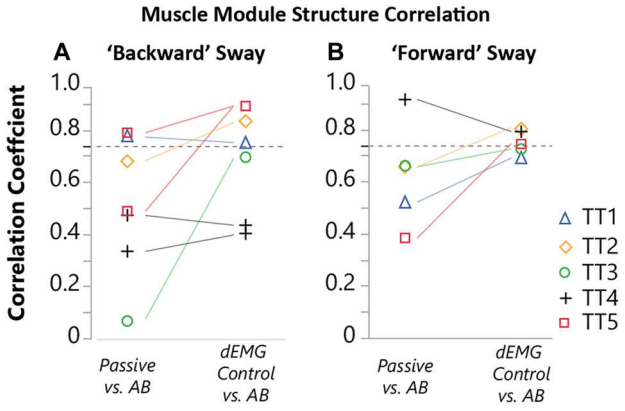

Fig. 6. Muscle module structure comparison between TT and AB participants. We compared correlation coefficients of muscle module structures from individual TT participants with average AB muscle module structure. Module correlation coefficient from individual transtibial amputee participants using either passive or dEMG-controlled device compared with the average AB module structure for all (**A**) "backward" and (**B**) "forward" labeled muscle. The dashed line indicates the threshold for significant correlation (0.735).

CoP measure is a common measure related to postural control, where CoP excursion will begin in anticipation of an oncoming disturbance, followed by changes in CoM excursion (*23*). This lack of symmetry in interlimb CoP excursion from amputees while using a passive prosthetic device is, in part, a result of lack of active ankle joint control and has been observed in a variety of tasks (*3*, *39*, *49*). Not only were participants capable of synchronizing interlimb CoP excursion using dEMG control, but they also decreased intact limb reliance during the push condition, as evidenced by reduced CoP excursion in the ML direction (Fig. 2D). Last, discrepancies in homologous joints excursions between limbs largely disappeared when participants used the dEMG control (Figs. 3 and 4). This signals a significant shift in TT individuals toward a normative postural control strategy. Typically, symmetric joint excursions are ubiquitous in the evaluation of postural control strategies because only kinematics from a single leg are reported. We expect that inherent differences in dynamics between amputees' intact limb and dEMG-controlled prosthesis may be an obstacle to interlimb symmetry; thus, it would be interesting to investigate whether tuning of active and passive prosthetic parameters results in greater symmetry using this control. Here, we present results demonstrating a potentially normative postural control strategy used by amputees wearing a robotic prosthetic ankle joint.

We noticed improvements in standing stability and the overall postural control strategies used by participants when using the dEMG control. Participants struggled to maintain standing balance under the push condition while using their passive device, as evidenced by the need for multiple steps or use of the safety rails on the perturbation platform. When using the dEMG control, participants were able to move their CoM position farther against the perturbation, resulting in no steps for nearly all participants (Fig. 4C). It is possible that this increased excursion of CoM was made possible by the dorsiflexion torque generated with the dEMG-controlled prosthetic ankle compared with the lack of dorsiflexion torque from individuals' passive devices. This improvement in stability was also evidenced by two postural control strategies in the dEMG control. TT1, TT2, and TT3 all used an ankle joint strategy, although TT4 and TT5 used a "mixed" strategy; however, it is important to note that these strategies may not represent reliable subgroups given the limited number of participants. Ankle joint, hip joint, and mixed strategies are well-observed postural control strategies used by individuals to maintain standing balance, where hip and mixed strategies are typically used during larger perturbations compared with ankle joint strategy (*52*). The use of an ankle joint strategy by TT1 to TT3 demonstrates increased capacity of these individuals to handle larger perturbations using dEMG control. Although only present for two individuals, TT4 and TT5's use of a mixed strategy suggests that this perturbation was still challenging while using the dEMG control. However, TT4 completed all trials with no steps or use of guard rails, demonstrating improved stability compared with using their daily passive device. TT5 was the only participant without improvements in compensatory steps; however, TT5 still significantly shifted their postural control strategy and incorporated the prosthesis ankle in the postural control. Because we did not force participants to adopt a specific strategy in this task and because the expected perturbation task was untrained, this suggests that this symmetric interlimb behavior adopted by TT5 while using the dEMG control potentially provided some functional benefit despite the lack of improvement in compensatory steps. It is possible that, given additional direct exposure with the expected perturbation task, more functional improvements could be observed, because training with this task directly has shown notable stability improvements in other populations (*24*, *53*). Our previous study had also shown that amputees adopt various learning strategies when using dEMG control in a virtual environment (*27*); thus, we plan to investigate improvements during training in the future to understand the potential differences in learning rates across amputees that could further explain this result.

Through systematic evaluation of neuromuscular coordination strategy via muscle module analysis, we witnessed drastic adaptation in neuromuscular control toward normative patterns (observed in individuals without limb amputations) with trained use of dEMG control. As far as the authors are aware, this is some of the first evidence to demonstrate near-normative neuromuscular control from previously antagonistic residual muscle in coordination with intact muscle groups after restoring the biomechanical influence of residual muscles through dEMG prosthesis ankle control. Compared with using their daily passive devices, amputees grouped muscle activations of intact and residual muscles using dEMG control of the prosthetic ankle with similar structures to AB individuals. Individual analysis highlighted how this shift was a result of reduction of number of muscle modules used to complete the voluntary postural sway task (fig. S3) and a reorganization of activation levels between muscles for improved symmetry between shank and thigh muscle activation. In addition, amputee users demonstrated a consistent, proficient pattern of muscle module recruitment using the dEMG control (Fig. 5) like AB participant behavior. In contrast with previous studies, participants did not require the use of artificial feedback about residual muscle activity (*32*), nor did they benefit from recent advances in amputation surgery that seek to improve proprioceptive feedback (*44*). It is possible that once the amputee participants visually "see" the consequence of residual muscle activation (ankle movement) and practice the dEMG control, the forward internal model that maps motor commands to prosthesis ankle state is

established, which enables amputee participants to estimate the state of the prosthesis directly by their neural control command without any real-time feedback from the prosthetic device (*54*). In addition, our included amputee participants might still maintain the intact neural pathways and neuromuscular coordination strategy before limb amputation. The reasons for our participants to shift the neuromuscular control when using passive devices are that the residual muscles do not have any biomechanical function after a limb amputation, and they need to produce compensation for task performance because one or more degrees of freedom in the lower limb are no longer available. dEMG control, however, restores the biomechanical influence of residual muscles, adding the missing degree of freedom (ankle joint) back to function. Therefore, after exposing amputee participants with dEMG-controlled prosthesis ankle for postural control in practice, it may be possible that they reused the existing postural control pathways and neural mechanisms from before their amputation for improved balance and postural stability. It would be an interesting future study to use neuroimaging techniques to investigate the neural control pathways in lower limb amputees after learning to use dEMG-controlled prostheses. In addition, this study limited the investigation of neuromuscular control and coordination in one task. It would be interesting to further investigate the neural coordination strategies for additional tasks on neuromuscular coordination strategies of amputees using dEMG control prosthetic ankles.

In summary, clinically, our study has demonstrated the significant improvement of postural control and stability and restoration of near-normative biomechanical and neuromuscular strategies during standing postural control tasks in TT individuals using dEMG control of a robotic ankle prosthesis. This control restores the biomechanical influence of residual muscles and reinstates the biomechanical resources (the missing ankle) in the lower-limb amputees for improved balance and postural stability. Technically, dEMG control enhances the functions of modern robotic prosthetic legs to actively assist postural stability and control, which has not been demonstrated by the existing autonomous control. We envision in the future a shared controller for robotic lower-limb prostheses, in which autonomous control assists cyclic, predictable locomotive tasks and dEMG control assists noncyclic, unpredictable tasks, such as dynamic postural control, to further improve the mobility of individuals with lower-limb amputations. Although the results in this study are promising, continued research efforts are still needed. First the participants in this study were active in daily life who were classified into K-3 level (active individuals capable of navigating most environments) in the Medicare Functional Classification Levels (*55*). A future study may include K-2 participants (limited community ambulators) to determine how these results can be generalized to the broader amputee population. It would be interesting to investigate the ability for amputees to use dEMG-controlled prosthesis under other common conditions of perturbation (translational and rotational platform movements, applying perturbations at other locations like the trunk or pelvis). Although we observed postural control improvements in the recruited amputee participants, it would be interesting to investigate individual participant improvement over training to understand the potential differences in dEMG control adaptation rates and other cognitive functions (such as cognitive load) across amputees. Last, future work should also include the use of a portable, motorized device (*14*, *56*) to evaluate the benefit of neural prosthesis control in the myriad of daily activities, in which amputees use their prosthetic devices.

MATERIALS AND METHODS

Participants

We recruited five individuals with unilateral transtibial amputation to participate in this study. All participants were male. This experimental protocol was approved at the University of North Carolina at Chapel Hill Institutional Review Board. Before participating in this study, each participant provided written consent after the nature and potential consequences of the study were explained. Information about the five TT participants is provided in Table 1. The average age of amputee participants was 43.4(±11.72) years. We also tested five AB participants to provide a reference for both biomechanics and neural behavior [average age: 39.2(±11.43) years]. All TT participants were active, community ambulators who wore their prosthesis at least 12 hours a day. No participants reported nerve damage or issues with sensation. TT5 had a notable comorbidity of dysvascular disease; however, no other participants reported any comorbidities. One participant was also an upper-limb amputee (TT2, shoulder disarticulation) and held the perturbation platform with a modified grip.

Pneumatic actuated ankle prosthesis

For this study, we fit a pneumatically actuated ankle prosthesis for each TT participant. Each participant fit their daily prosthetic socket to the pneumatic ankle, and the alignment for each participant was set by trained prosthetist while the prosthesis was locked in a 90° position. This prosthetic ankle contained four pneumatic artificial muscles (PAMs), two placed anteriorly to generate dorsiflexion moments and two posteriorly for plantarflexion moments. These PAMs were used to produce similar force-length dynamics of intact musculature and were actuated using EMG magnitude taken from the envelope of residual muscle activity. More details on the ankle prosthesis can be found in (*57*).

dEMG control

In this study, we took the envelope of previously antagonistic residual muscle activity to drive prosthetic ankle dynamics directly and continuously. We calculated the envelope of the residual tibialis anterior (rTA) and residual lateral gastrocnemius (rLGAS) activity in real time (dSPACE, CLP-1103, 0 to 10 V output) to generate a smoothed control signal. We processed the residual muscle activity in real time by first applying a high-pass filter (100 Hz, second-order Butterworth) to reduce the effect from potential signal artifacts. Our real-time filtering then rectified the EMG signal and applied a low-pass filter (2 Hz, second-order Butterworth). Our system then sent the filtered control signal from each muscle to the pressure regulators responsible for generating pressure proportional to the input voltage (0 to 10 V for 0 to 90 psi). We applied a gain to each input control signal at the beginning of each session such that a maximum contraction from each muscle resulted in a control signal between 9 and 10 V. To establish a set ankle stiffness, we applied baseline air pressure of approximately 2 V for each participant. This process is detailed in (*39*) as well as in the Supplementary Materials.

Experimental protocol

Similar to our procedure in previous work (*39*), we introduced TT participants to the pneumatic ankle with several acclimation trials before the start of training and evaluation. After acclimation, our study consisted of a minimum of three training sessions and two evaluation sessions. The details of this acclimation and training can be found in the Supplementary Materials.

To evaluate the ability of amputees to produce APAs under expected perturbation using dEMG control, we developed a platform capable of delivering expected perturbations in two directions: push and pull (Figs. 1 and 2A). In this setup, we asked each participant to hold a handlebar placed at shoulder level while standing in a relaxed posture. We placed a light-emitting diode (LED) strip at the eye level of the participant. For the participant to know the perturbation timing, we switched off the LED strip 0.6 s before the electromagnet was released via two relays (5 V, Parallax, CA, USA) controlled using LabVIEW (NI, Austin, TX, USA). In this setup, the perturbation was delivered by a hanging weight that was connected to the handlebars by two cords via a series of pulleys such that the vertical force of the weight was translated into a horizontal force on the handlebars. We placed an electromagnet in series with one of the cords to control its connection with the weight. Thus, when the electromagnet was released, all weight was transferred horizontally, causing a force in the direction of the cord that remained attached to the handlebar. The location of the electromagnet was switched on the basis of the desired perturbation direction (push or pull). We placed one load cell on each side of the handlebar to measure the force each participant applied before and during perturbation. A trial was removed from the analysis if participants applied force to the handlebar before the light switch. Before each repetition, we visually confirmed the participant's stance to ensure that they had a vertical, relaxed posture with both feet placed symmetrically and shoulder-width apart. We repeated each perturbation five times for each condition. We provided each participant with five practice trials for each condition before the beginning of testing to familiarize them with the task. The order of testing each weight and direction was randomized before the start of the evaluation session. The magnitude of the perturbation was chosen on the basis of pilot testing because the perturbation magnitude was sufficiently difficult that amputee participants would potentially be unable to maintain balance during either the push or pull condition. We conducted this evaluation using 10% of the participant's BW as the perturbation magnitude in both a pull and a push direction. On separate days, we then evaluated dEMG control with both perturbation trials and the trained activities. We conducted the same evaluation on a separate day with participants using their daily device. The order of evaluation between devices was randomized, where TT1, TT2, and TT3 conducted the passive evaluation after the training and evaluation with the dEMG control. TT4 and TT5 conducted the passive evaluation before training and evaluation with the dEMG-controlled ankle.

Measurements

During all sessions, we collected EMG activities from intact and residual limb thigh and shank muscles. We placed EMG sensors (Motion Lab Systems, MA-420, Gainx20, Baton Rouge, LA, USA) on the following muscles: intact tibialis anterior, intact lateral gastrocnemius, intact soleus, intact and residual limb rectus femoris, intact and residual limb vastus lateralis, and intact and residual limb biceps femoris. We determined the location of muscle via palpation and anatomical landmarks (*58*). For rTA and rLGAS, which are inside of the prosthetic socket, we placed low-profile EMG sensors (Neuroline 715, 1 mm in height, Ballerup, Denmark). We located muscles via palpation while participants contracted and relaxed muscles (*59*). When residual muscle flexion was difficult to locate via palpation, we placed EMG sensors on the basis of anatomical landmarks. We then iteratively shifted EMG sensor location to determine whether other locations provided improved the observed signal-to-noise ratio. We routed cables to avoid bony landmarks and connected them to pre-amplifiers (Motion Lab Systems, MA-412, Gainx20, Baton Rouge, LA, USA) outside of the prosthetic socket. We connected all sensors to an amplifier (MA300-XVI, Gain x1000).

In each session, we collected ground reaction forces (GRF) and moments under each foot using an instrumented split-belt treadmill (1000 Hz, Bertec Corp., Columbus, OH, USA). CoP values were calculated under each foot using GRF and moments. We calculated overall CoP using the weighted average under each foot, weighted by GRF (*39*). We collected full-body kinematics (100 Hz, 43 markers, Vicon, Oxford, UK). We calculated CoM position using the analysis software (Visual 3D, C-Motion Inc., Germantown, MD, USA). We low-pass–filtered data from the treadmill (GRF and CoP) (20 Hz, fourth-order Butterworth). From the perturbation setup, we collected loading data from the handlebar via two tension load cells (Omega, Stamford, CT, USA) placed on the anterior and posterior sides. We recorded the control signal sent to each relay for light switch and electromagnet from the same sampling rate as our split-belt treadmill.

Expected perturbation data analysis

We processed data offline using MATLAB (MathWorks, Natick, MA, USA). For perturbation trials, we extracted and windowed each perturbation to 600 ms before load release and 2000 ms after release. To evaluate participant stability during each release perturbation, we selected the CoM excursion, CoP excursion, and ankle joint torque during each condition. For each repetition, we calculated the average of each measure from 600 to 500 ms before perturbation. We then subtracted this average value from each measure during each perturbation. We took the average of the first five recorded trials for each condition, each device, and each participant. We plotted the time series of each selected measure to compare behavior between the AB control, TT Passive, and TT dEMG control condition behavior. We plotted the push condition response because this was the most challenging condition for all participants (as evidenced by frequent stepping responses required by TT participants with their passive device). For quantitative analysis, we selected two time points from each repetition to understand the anticipatory and compensatory postural responses. For anticipatory responses, we extracted the value of each measure at the moment of load release ($t = 0$ s). Because the perturbation required participants to hold the load after release, we calculated the average value of each measure for 1000 to 2000 ms after the load release, termed hold. We selected this time to capture the long-term behavior of participants, where most TT participants using their passive device initiated and finished compensatory movements (steps, using guard rails) during this time window.

To understand joint level strategies of participants when using their passive prosthesis compared with dEMG control, we evaluated

the ankle, knee, and hip joint excursions during all perturbation repetitions with the same windowing described above. We subtracted the average joint angle of 600 to 500 ms before load release from the full time series. For evaluation, we then extracted values from "release" and hold time points.

For qualitative analysis of full-body strategies to maintain balance, we qualitatively evaluated the combination of joint angle excursions from each participant using the dEMG control by observing two distinct joint excursions strategies. For three participants, we identified primarily an "ankle strategy" when responding to the disturbance (where the hip and knee joint excursions did not exceed 2° in either direction). For the remaining two participants, we noticed a "mixed strategy" where participants moved all joints more than 2° for each joint simultaneously. We empirically defined these boundaries of excursions for strategies based on previous study of standing balance under perturbation (*60*). During each condition, we observed the number of instances where participants could not maintain balance. They either held onto the handlebar until it reached either the forward or backward stop or took a compensatory step (Fig. 4C). We counted the number of these situations for each condition.

Voluntary postural sway (muscle module) data analysis

For the voluntary postural sway, we processed all data offline using MATLAB. We selected the first trial from the final evaluation day. We first low-pass–filtered all data from the instrumented split-belt treadmill (20 Hz, second-order Butterworth). We calculated CoP in the anterior-poster (CoP_{AP}) direction using GRF and moment data from the treadmill (*61*). We windowed each individual sway, selecting the forward-most extremes of CoP_{AP} as the beginning and end of the sway. For each trial, we first removed any sways where the participant was unable to maintain balance and required a step forward or backward. For the muscle module analysis, we selected the middle 12 sways (*45*) from the remaining data. For evaluation of kinematic and kinetic variables, we included all sways from the remaining data.

We postprocessed EMG data by high-pass filtering (35 Hz, third-order Butterworth), rectifying, then low-pass filtering (40 Hz, third-order Butterworth) (*62*). We down-sampled the collected EMG by averaging data into 50-ms time bins (*62*). We then concatenated EMG data from all sways for each condition and participant, generating data matrices of m (number of muscles) × b (number of bins) (*62*). We did not time normalize EMG data, which resulted in data matrices of different sizes between participants (*62*). EMG matrices for each condition and participant contained a minimum of 700 data points. We normalized EMG values of each muscle vector by a maximum voluntary contraction (MVC) for each muscle trial gathered at the beginning of each testing session. If we observed a muscle activation during the voluntary postural sway task that was larger than the collected MVC, then we normalized the given muscle vector by this value instead. We did this separately for each condition and participant. We then scaled each muscle vector to have unit variance in the order that equal weighting was applied to each muscle during the muscle mode analysis. After muscle module extraction, we removed this scaling for each muscle vector.

Muscle module extraction

We extracted muscle modules from each condition and participant separately using nonnegative matrix factorization (NNMF) (*62*). NNMF has been used in numerous studies evaluating muscle module presence in various tasks and patient populations (*62*–*64*). NNMF extracts muscle modules with the assumption that individual activity from muscles, $V_{b,m}$, is the result of the multiplication of groupings of muscles, $H_{n,m}$, with a module recruitment coefficient, $W_{b,n}$

$$V_{b,m} = W_{b,n} * H_{n,m} \quad (1)$$

where $V_{b,m}$ is the reconstructed EMG activity of all m muscles and n represents the number of muscle modules used to reconstruct the original EMG activity. Using this model, groupings of muscle modules, $H_{n,m}$, are fixed, whereas the activation of these modules, $W_{b,n}$, varies with time. Thus, various motor behaviors can be generated through the combination of the activation of one or more muscle modules. We determined the number of muscle modules required to sufficiently reconstruct the original EMG data using identical criteria to the previous study (*62*). The exact details are available in the Supplementary Materials.

Muscle module analysis

We analyzed the similarity between muscle modules across conditions. We first empirically grouped muscle modules into three groups based on the activation coefficient profile. We observed three common muscle module activation profiles labeled Forward, Backward, and "Tonic" modules. We characterized Forward modules by two peaks in the activation profile for the given muscle modules located at the forward-most part of the postural sway cycle (0 and 100% of sway cycle). Similarly, modules were labeled Backward if the activation profile contained a single peak, where the peak was located at the backward most part of the postural sway (50% of the sway cycle) (Fig. 5). Third, we labeled muscle modules that contained a constant activation of muscle across the sway cycle as Tonic muscle modules. Across all conditions and participants, we observed one Tonic muscle module (TT1 dEMG control) and two additional muscle modules with multiple activation coefficient peaks (TT1 and TT2 passive), which we did not label (Supplementary Materials and fig. S4).

We determined similarity between muscle module structures within groupings (passive versus AB, dEMG control versus AB) by calculating the correlation coefficient between muscle module arrays across conditions (*65*). Specifically, for each participant, we calculated the correlation coefficient between each Forward muscle module pretraining with the averaged Forward muscle module of all AB participants. We repeated this for Backward sways as well. Significant correlations between muscle module structure were correlations greater than 0.735, which corresponded to significance level of previous muscle module study (*66*, *67*) (further detail can be found in the Supplementary Materials).

Statistical analysis

We conducted statistical analysis of the data using statistical software (JMP, SAS, Cary, NC, USA). We used two-way analyses of variance (ANOVAs) for CoP excursion and joint angle excursions at release and hold time points with device (passive versus dEMG control) and limb (intact versus residual) as the main and interaction effects. We compared CoM and mediolateral CoP behavior between AB and TT participants using each device (AB versus passive, AB versus dEMG control) using one-way ANOVA. We further compared those same outcome measures with TT

participants between device conditions (passive versus dEMG control) using one-way ANOVA. For each analysis, we included participant as a random effect. We conducted pair-wise comparisons using Tukey's post hoc test. We evaluated whether each analysis failed normality assumptions using a Shapiro-Wilk test of studentized residual distribution. We also evaluated whether each analysis failed equal variance assumption using Levene's test for equal variance. When an analysis failed the normality or variance assumption, we conducted nonparametric Wilcoxon tests. We set a threshold for significance at $a = 0.05$ for all tests. The tests that failed assumptions required for parametric tests can be seen in the Supplementary Material (table S3) as well as excluded trials and justification. We did not remove any outliers from our data.

Supplementary Materials

This PDF file includes:
Methods
Figs. S1 to S6
Tables S1 to S3

Other Supplementary Material for this manuscript includes the following:
MDAR Reproducibility Checklist

REFERENCES AND NOTES

1. F. B. Horak, Postural orientation and equilibrium: What do we need to know about neural control of balance to prevent falls? *Age Ageing* **35**, ii7–ii11 (2006).
2. C. Curtze, A. L. Hof, K. Postema, B. Otten, The relative contributions of the prosthetic and sound limb to balance control in unilateral transtibial amputees. *Gait Posture* **36**, 276–281 (2012).
3. D. F. Rusaw, S. Ramstrand, Validation of the Inverted Pendulum Model in standing for transtibial prosthesis users. *Clin. Biomech. (Bristol, Avon)* **31**, 100–106 (2016).
4. M. J. Nederhand, E. H. Van Asseldonk, H. van der Kooij, H. S. Rietman, Dynamic Balance Control (DBC) in lower leg amputee subjects; contribution of the regulatory activity of the prosthesis side. *Clin. Biomech. (Bristol, Avon)* **27**, 40–45 (2012).
5. P. X. Ku, N. A. A. Osman, W. A. B. W. Abas, Balance control in lower extremity amputees during quiet standing: A systematic review. *Gait Posture* **39**, 672–682 (2014).
6. A. H. Vrieling, H. G. van Keeken, T. Schoppen, E. Otten, A. L. Hof, J. P. K. Halbertsma, K. Postema, Balance control on a moving platform in unilateral lower limb amputees. *Gait Posture* **28**, 222–228 (2008).
7. C. K. Wong, C. C. Chen, W. M. Blackwell, R. T. Rahal, S. A. Benoy, Balance ability measured with the Berg balance scale: A determinant of fall history in community-dwelling adults with leg amputation. *J. Rehabil. Med.* **47**, 80–86 (2015).
8. N. Steinberg, A. Gottlieb, I. Siev-Ner, M. Plotnik, Fall incidence and associated risk factors among people with a lower limb amputation during various stages of recovery–a systematic review. *Disabil. Rehabil.* **41**, 1778–1787 (2019).
9. W. Miller, A. Deathe, A prospective study examining balance confidence among individuals with lower limb amputation. *Disabil. Rehabil.* **26**, 875–881 (2004).
10. W. C. Miller, A. B. Deathe, M. Speechley, J. Koval, The influence of falling, fear of falling, and balance confidence on prosthetic mobility and social activity among individuals with a lower extremity amputation. *Arch. Phys. Med. Rehabil.* **82**, 1238–1244 (2001).
11. A. Tatarelli, M. Serrao, T. Varrecchia, L. Fiori, F. Draicchio, A. Silvetti, S. Conforto, C. de Marchis, A. Ranavolo, Global muscle coactivation of the sound limb in gait of people with transfemoral and transtibial amputation. *Sensors* **20**, 2543 (2020).
12. P. Mehryar, M. Shourijeh, T. Rezaeian, N. Iqbal, N. Messenger, A. A. Dehghani-Sanij, Changes in synergy of transtibial amputee during gait: A pilot study. in *2017 IEEE EMBS International Conference on Biomedical & Health Informatics (BHI)*, 2017: IEEE, pp. 325–328.
13. N. Vanicek, S. Strike, L. McNaughton, R. Polman, Postural responses to dynamic perturbations in amputee fallers versus nonfallers: A comparative study with able-bodied subjects. *Arch. Phys. Med. Rehabil.* **90**, 1018–1025 (2009).
14. S. Au, M. Berniker, H. Herr, Powered ankle-foot prosthesis to assist level-ground and stair-descent gaits. *Neural Netw.* **21**, 654–666 (2008).
15. F. Sup, A. Bohara, M. Goldfarb, Design and control of a powered transfemoral prosthesis. *Int. J. Robot. Res.* **27**, 263–273 (2008).
16. T. Elery, S. Rezazadeh, C. Nesler, R. D. Gregg, Design and validation of a powered knee–ankle prosthesis with high-torque, low-impedance actuators. *IEEE Trans. Robot.* **36**, 1649–1668 (2020).
17. A. F. Azocar, L. M. Mooney, L. J. Hargrove, E. J. Rouse, Design and characterization of an open-source robotic leg prosthesis. in *2018 7th IEEE International Conference on Biomedical Robotics and Biomechatronics (Biorob)*, 2018: IEEE, pp. 111–118.
18. T. Lenzi, M. Cempini, L. Hargrove, T. Kuiken, Design, development, and testing of a lightweight hybrid robotic knee prosthesis. *Int. J. Robot. Res.* **37**, 953–976 (2018).
19. M. Liu, F. Zhang, P. Datseris, H. Huang, Improving finite state impedance control of active-transfemoral prosthesis using dempster-shafer based state transition rules. *J. Intell. Robot. Syst.* **76**, 461–474 (2014).
20. M. F. Eilenberg, H. Geyer, H. Herr, Control of a powered ankle–foot prosthesis based on a neuromuscular model. *IEEE Trans. Neural Syst. Rehabil. Eng.* **18**, 164–173 (2010).
21. S. K. Au, J. Weber, H. Herr, Powered Ankle--foot prosthesis improves walking metabolic economy. *IEEE Trans. Robot.* **25**, 51–66 (2009).
22. M. J. Santos, N. Kanekar, A. S. Aruin, The role of anticipatory postural adjustments in compensatory control of posture: 1. Electromyographic analysis. *J. Electromyogr. Kinesiol.* **20**, 388–397 (2010).
23. M. J. Santos, N. Kanekar, A. S. Aruin, The role of anticipatory postural adjustments in compensatory control of posture: 2. Biomechanical analysis. *J. Electromyogr. Kinesiol.* **20**, 398–405 (2010).
24. N. Kanekar, A. S. Aruin, Improvement of anticipatory postural adjustments for balance control: Effect of a single training session. *J. Electromyogr. Kinesiol.* **25**, 400–405 (2015).
25. S. Jagdhane, N. Kanekar, A. S. Aruin, The effect of a four-week balance training program on anticipatory postural adjustments in older adults: A pilot feasibility study. *Curr. Aging Sci.* **9**, 295–300 (2016).
26. D. Farina, I. Vujaklija, R. Brånemark, A. M. J. Bull, H. Dietl, B. Graimann, L. J. Hargrove, K.-P. Hoffmann, H. H. Huang, T. Ingvarsson, H. B. Janusson, K. Kristjánsson, T. Kuiken, S. Micera, T. Stieglitz, A. Sturma, D. Tyler, R. F. F. Weir, O. C. Aszmann, Toward higher-performance bionic limbs for wider clinical use. *Nat. Biomed. Eng.*, 473–485 (2021).
27. A. Fleming, S. Huang, H. Huang, Proportional myoelectric control of a virtual inverted pendulum using residual antagonistic muscles: Toward voluntary postural control. *IEEE Trans. Neural Syst. Rehabil. Eng.* **27**, 1473–1482 (2019).
28. H. Huang, F. Zhang, L. J. Hargrove, Z. Dou, D. R. Rogers, K. B. Englehart, Continuous locomotion-mode identification for prosthetic legs based on neuromuscular–mechanical fusion. *IEEE Trans. Biomed. Eng.* **58**, 2867–2875 (2011).
29. H. Huang, T. A. Kuiken, R. D. Lipschutz, A strategy for identifying locomotion modes using surface electromyography. *IEEE. Trans. Biomed. Eng.* **56**, 65–73 (2009).
30. L. J. Hargrove, A. M. Simon, A. J. Young, R. D. Lipschutz, S. B. Finucane, D. G. Smith, T. A. Kuiken, Robotic leg control with EMG decoding in an amputee with nerve transfers. *N. Engl. J. Med.* **369**, 1237–1242 (2013).
31. A. Fleming, N. Stafford, S. Huang, X. Hu, D. P. Ferris, H. H. Huang, Myoelectric control of robotic lower limb prostheses: A review of electromyography interfaces, control paradigms, challenges and future directions. *J. Neural Eng.* **18**, 10.1088/1741-2552/ac1176, (2021).
32. S. Huang, J. P. Wensman, D. P. Ferris, Locomotor adaptation by transtibial amputees walking with an experimental powered prosthesis under continuous myoelectric control. *IEEE Trans. Neural Syst. Rehabil. Eng.* **24**, 573–581 (2016).
33. C. D. Hoover, G. D. Fulk, K. B. Fite, Stair ascent with a powered transfemoral prosthesis under direct myoelectric control. *IEEE/ASME Trans. Mechatron.* **18**, 1191–1200 (2012).
34. J. Wang, O. A. Kannape, H. M. Herr, Proportional EMG control of ankle plantar flexion in a powered transtibial prosthesis. *IEEE Int. Conf. Rehabil. Robot.* **2013**, 6650391 (2013).
35. S. Huang, H. Huang, Voluntary control of residual antagonistic muscles in transtibial amputees: Feedforward ballistic contractions and implications for direct neural control of powered lower limb prostheses. *IEEE Trans. Neural. Syst. Rehabil. Eng.* **26**, 894–903 (2018).
36. B. Chen, Q. Wang, L. Wang, Promise of using surface EMG signals to volitionally control ankle joint position for powered transtibial prostheses. *Annu. Int. Conf. IEEE Eng. Med. Biol. Soc.* **2014**, 2545–2548 (2014).
37. C. D. Hoover, G. D. Fulk, K. B. Fite, The design and initial experimental validation of an active myoelectric transfemoral prosthesis. *J. Med. Dev.* **6**, 011005 (2012).
38. T. R. Clites, H. M. Herr, S. S. Srinivasan, A. N. Zorzos, M. J. Carty, The Ewing amputation: The first human implementation of the agonist-antagonist myoneural interface. *Plast. Reconstr. Surg. Glob. Open* **6**, e1997 (2018).
39. A. Fleming, S. Huang, E. Buxton, F. Hodges, H. H. Huang, Direct continuous electromyographic control of a powered prosthetic ankle for improved postural control after guided physical training: A case study. *Wearable Technol.* **2**, e3 (2021).
40. S. Huang, D. P. Ferris, Muscle activation patterns during walking from transtibial amputees recoded within the residual limb-prosthetic interface. *J. Neuroeng. Rehabil.* **9**, 55 (2012).

41. E. C. Wentink, E. C. Prinsen, J. S. Rietman, P. H. Veltink, Comparison of muscle activity patterns of transfemoral amputees and control subjects during walking. *J. Neuroeng. Rehabil.* **10**, 87 (2013).
42. S. Huang, H. Huang, Voluntary control of residual antagonistic muscles in transtibial amputees: Reciprocal activation, coactivation, and implications for direct neural control of powered lower limb prostheses. *IEEE Trans. Neural Syst. Rehabil. Eng.* **27**, 85–95 (2019).
43. J. A. Dawley, K. B. Fite, G. D. Fulk, EMG control of a bionic knee prosthesis: Exploiting muscle co-contractions for improved locomotor function. *IEEE Int. Conf. Rehabil. Robot.* **2013**, 6650389 (2013).
44. T. R. Clites, M. J. Carty, J. B. Ullauri, M. E. Carney, L. M. Mooney, J. F. Duval, S. S. Srinivasan, H. M. Herr, Proprioception from a neurally controlled lower-extremity prosthesis. *Sci. Transl. Med.* **10**, eaap8373 (2018).
45. A. Danna-dos-Santos, K. Slomka, V. M. Zatsiorsky, M. L. Latash, Muscle modes and synergies during voluntary body sway. *Exp. Brain Res.* **179**, 533–550 (2007).
46. A. d'Avella, E. Bizzi, Shared and specific muscle synergies in natural motor behaviors. *Proc. Natl. Acad. Sci. U.S.A.* **102**, 3076–3081 (2005).
47. L. H. Ting, H. J. Chiel, R. D. Trumbower, J. L. Allen, J. L. McKay, M. E. Hackney, T. M. Kesar, Neuromechanical principles underlying movement modularity and their implications for rehabilitation. *Neuron* **86**, 38–54 (2015).
48. A. S. Aruin, M. L. Latash, The role of motor action in anticipatory postural adjustments studied with self-induced and externally triggered perturbations. *Exp. Brain Res.* **106**, 291–300 (1995).
49. A. Aruin, J. Nicholas, M. L. Latash, Anticipatory postural adjustments during standing in below-the-knee amputees. *Clin. Biomech. (Bristol, Avon)* **12**, 52–59 (1997).
50. D. Piscitelli, A. Falaki, S. Solnik, M. L. Latash, Anticipatory postural adjustments and anticipatory synergy adjustments: Preparing to a postural perturbation with predictable and unpredictable direction. *Exp. Brain Res.* **235**, 713–730 (2017).
51. R. Gailey, I. Gaunaurd, M. Raya, N. Kirk-Sanchez, L. M. Prieto-Sanchez, K. Roach, Effectiveness of an evidence-based amputee rehabilitation program: A pilot randomized controlled trial. *Phys. Ther.* **100**, 773–787 (2020).
52. F. B. Horak, L. M. Nashner, Central programming of postural movements: Adaptation to altered support-surface configurations. *J. Neurophysiol.* **55**, 1369–1381 (1986).
53. A. S. Aruin, N. Kanekar, Y.-J. Lee, M. Ganesan, Enhancement of anticipatory postural adjustments in older adults as a result of a single session of ball throwing exercise. *Exp. Brain Res.* **233**, 649–655 (2015).
54. C. D. Frith, S. J. Blakemore, D. M. Wolpert, Abnormalities in the awareness and control of action. *Philos. Trans. R. Soc. Lond. B Biol. Sci.* **355**, 1771–1788 (2000).
55. R. S. Gailey, K. E. Roach, E. B. Applegate, B. Cho, B. Cunniffe, S. Licht, M. Maguire, M. S. Nash, The amputee mobility predictor: An instrument to assess determinants of the lower-limb amputee's ability to ambulate. *Arch. Phys. Med. Rehabil.* **83**, 613–627 (2002).
56. S. Upadhye, C. Shah, M. Liu, G. Buckner, H. H. Huang, A Powered Prosthetic Ankle Designed for Task Variability–A Concept Validation. presented at the (2021) IEEE/RSJ International Conference on Intelligent Robots and Systems (IROS).
57. S. Huang, J. P. Wensman, D. P. Ferris, An experimental powered lower limb prosthesis using proportional myoelectric control. *J. Med. Dev.* **8**, 024501 (2014).
58. A. O. Perotto, *Anatomical Guide for the Electromyographer: The Limbs and Trunk* (Charles C Thomas Publisher, 2011).
59. S. Huang, D. P. Ferris, Muscle activation patterns during walking from transtibial amputees recorded within the residual limb-prosthetic interface. *J. Neuroeng. Rehabil.* **9**, 55 (2012).
60. C. Runge, C. Shupert, F. Horak, F. Zajac, Ankle and hip postural strategies defined by joint torques. *Gait Posture* **10**, 161–170 (1999).
61. D. A. Winter, F. Prince, J. Frank, C. Powell, K. F. Zabjek, Unified theory regarding A/P and M/L balance in quiet stance. *J. Neurophysiol.* **75**, 2334–2343 (1996).
62. A. Sawers, J. L. Allen, L. H. Ting, Long-term training modifies the modular structure and organization of walking balance control. *J. Neurophysiol.* **114**, 3359–3373 (2015).
63. D. J. Clark, L. H. Ting, F. E. Zajac, R. R. Neptune, S. A. Kautz, Merging of healthy motor modules predicts reduced locomotor performance and muscle coordination complexity post-stroke. *J. Neurophysiol.* **103**, 844–857 (2010).
64. J. L. Allen, J. L. McKay, A. Sawers, M. E. Hackney, L. H. Ting, Increased neuromuscular consistency in gait and balance after partnered, dance-based rehabilitation in Parkinson's disease. *J. Neurophysiol.* **118**, 363–373 (2017).
65. S. A. Chvatal, J. M. Macpherson, G. Torres-Oviedo, L. H. Ting, Absence of postural muscle synergies for balance after spinal cord transection. *J. Neurophysiol.* **110**, 1301–1310 (2013).
66. S. A. Safavynia, L. H. Ting, Task-level feedback can explain temporal recruitment of spatially fixed muscle synergies throughout postural perturbations. *J. Neurophysiol.* **107**, 159–177 (2012).
67. J. Frère, F. Hug, Between-subject variability of muscle synergies during a complex motor skill. *Front. Comput. Neurosci.* **6**, 99 (2012).

Acknowledgments: We would like to thank L. Ting and L. Resnik for valuable suggestions on this study. We would also like to thank B. Kim and J. Skigen for help in assisting with initial prototyping of the perturbation platform. We would like to thank J. Stallrich for suggestions on statistical analysis as well as J. Berman for assistance proofreading the manuscript. **Funding:** Funding for this research project was received from NIH F31HD101285, NIH R01HD110519, and NSF1954587. **Author contributions:** A.F. and H.H. contributed to the conceptualization and methodology for the experiments. A.F. contributed to the design of the perturbation platform. A.F. and W.L. carried out the experiments. A.F. analyzed the data. A.F. and H.H. prepared the manuscript. All authors revised and approved the final manuscript. **Competing interests:** The authors declare that they have no competing interests. **Data and materials availability:** All data needed to evaluate the conclusions in the paper are present in the paper or the Supplementary Materials. All data are available at https://osf.io/8WFA7/.

Submitted 31 October 2022
Accepted 20 September 2023
Published 18 October 2023
10.1126/scirobotics.adf5758

Science Robotics

Neural prosthesis control restores near-normative neuromechanics in standing postural control

Aaron Fleming, Wentao Liu, and He (Helen) Huang

Sci. Robot. **8** (83), eadf5758. DOI: 10.1126/scirobotics.adf5758

Science Robotics (ISSN 2470-9476) is published by the American Association for the Advancement of Science. 1200 New York Avenue NW, Washington, DC 20005. The title *Science Robotics* is a registered trademark of AAAS.